6.

ADDIS ABABA UNIVERSITY

SCHOOL OF GRADUATE STUDIES

Geophysical Investigation of the Crustal Structure Beneath Metehara, Main Ethiopian Rift.

By

ADDISU GUTA

JUNE 2010
ADDIS ABABA

6

Geophysical Investigation of the Crustal Structure Beneath Metehara, Main Ethiopian Rift.

By

ADDISU GUTA
(Department of Earth Science)

Approved By Board of Examiners

Advisor	
Examiner (1)	
Examiner (2)	
Chair man	

Geophysical Investigation of the Crustal Structure Beneath Metehara, Main Ethiopian Rift.

By

ADDISU GUTA

A THESIS SUBMITTED TO THE SCHOOL OF GRADUATE STUDIES OF THE ADDIS ABABA UNIVERSITY IN PARTIAL FULFILLMENT OF THE REQUIREMENTS FOR THE OF MASTERS OF SCIENCE IN EXPLORATION GEOPHYSICS

Department of Earth Sciences

ADDIS ABABA UNIVERSITY

JUNE 2010

ADDIS ABABA

ACKNOWEDGEMENTS

I would first and prime like to pay tribute to the Almighty God for being on my side in all my accomplishments with His endless love.

Next my heartfelt thanks go to my Advisor, **Dr. Tilahun Mammo** for his productive counsel, restless and guidance with understanding through out the course of the study.

My genuine deepest thanks also go to all my families, especially to my Mama and sweet brother Yared and for his best "Rome!" for their continuous encouragement and support. I would like to express my special credit to all of my class mate friends and my warm appreciation goes to Rukiya and her families for their moral and support throughout my academic work.

This research work was financed through the grant from AAU; Department of Earth sciences must be thanked for funding the research.

ABSTRACT

Analysis of the gravity data, with the help of the seismic refraction results (G.D. Mackenzile, H .Thybo and P .K .H .Maguire 2005) and Euler deaconvolution results also produced to simplify the modeling process of the study region and it was done to study the crurtal thickness variation under the subsurface layers of Metehara.

Which is located 39^0 30^{l} 48.340^{ll} to 40^0 59^{l} 27.600^{ll} E longitude and 8^0 48^{l} 15.120^{ll} to 9^0 28^{l} 41.268^{ll} N latitude as shown in Fig.1.1.The Bouguer gravity anomaly which shows the area of study relatively higher value with a strongly denser contour at the lower corner of S-E of the anomaly map.

The Gravity modeling constrained with seismic refraction and Euler deconvelutivn result, indicates a crurtal thickness of about 34.8 and 36.6km under selected profiles AB and MN respectively. The model also shows two highest dense bodies as mafic intrusions over profile AB.

TABLE OF CONTENTS

List of figures Pages

Table pages

CHAPTER-ONE

1. INTRODUCTION

1.1 Location

The area of the study ;Metehara ,regionally it is found in the eastern part of the Oromia regional state , which is located in the Main Ethiopia Rift System and bounded by **$39^0 30^{|} 48.340^{||}$ to $40^0 59^{|} 27.600^{||}$ E longitude and $8^0 48^{|} 15.120^{||}$ to $9^0 28^{|} 41.268^{||}$ N latitude** as shown in the figure bellow.

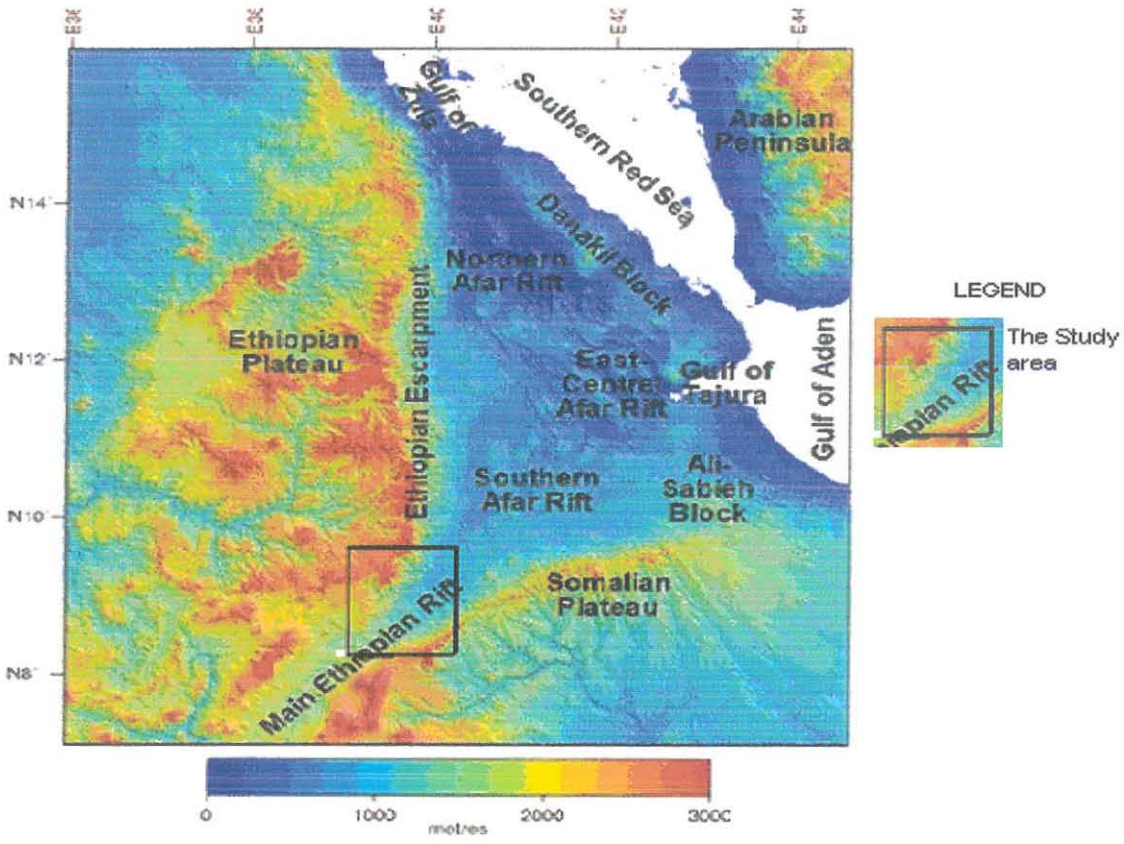

Figure 1.1 Digital elevation of the study area

1.2 Methodology

The methods involve using measured earth gravitational field to map subsurface variation with density. The basis of using variation in gravitational acceleration as a measure of density variations is that, the force of attraction between two masses is directly proportional to the product of two masses, and inversely proportional to the square of the distance between them. If the force of attraction experienced by the fixed mass can be measured carefully at different location on the earth, the change in this attraction can be related to mass of subsurface material. There are other aspects that affect the force of attraction experienced by the fixed mass, but this effect can be removed so that the residual variation can be related to sub surface distribution of density.

To facilitate the process computer software used including GEOSOFT software package for performing standard gravity correction and data modeling, Excel spread sheet for organizing data and, Sulfur 8 for editing and producing standard map. In addition, various enhancement and filtering techniques were conducted for better interpretation of the result.

1.3. General objective

The aim of this study is to **investigate the crustal structure in the Main Ethiopian rift, around Metehara** using gravity method.

1.3.1. Specific objectives:

- To determine the Moho depth of the study area.
- To set 2.5D model of the structure beneath the study area.
- To identify deep seated structures.

CHAPTER-TWO

2. GENERAL REGIONAL GEOLOGY

2.1 Geology of the Main Ethiopian Rift

The third arm of the Afar triple junction is the East African rift system. This extends through Ethiopia and Kenya and branches around the Tanzanian Craton before dying out in Mozambique. The northernmost part of the East African rift system is the Main Ethiopian Rift which opens out into the Afar Depression. It is bound to the north by the Ethiopian Plateau and to the south by the Somalian Plateau (e.g. Beyene & Abdelsalam, 2005).

Extension between the Nubian and Somalian plates beginning about 25Ma lead to rifting along the East African Rift system. Rifting across the southern part of the Main Ethiopian rift began about 18Ma and about 11Ma across the northern part of the rift when it propagated northwards across older Red Sea/Gulf of Aden structures to form the Afar triple junction

The Main Ethiopian rift is a central valley some 84km wide and is extending ESE-WNW at a rate of about 2.5mm/yr). The rift is bordered by large, discontinuous Miocene aged normal faults within the main rift are a series of right-stepping, en echelon Quaternary rift basins. These are typically about 20km wide and 60km long faulted magmatic segments and are embryonic oceanic spreading centers (Hayward and Ebinger, 1996; Manighetti et al, 1998 and Ebinger & Casey, 2001). The Miocene border faults are thought to be now inactive and extension focused along the magmatic segments (Ebinger & Casey, 2001; Casey et al, 2006; Keir et al, 2006).

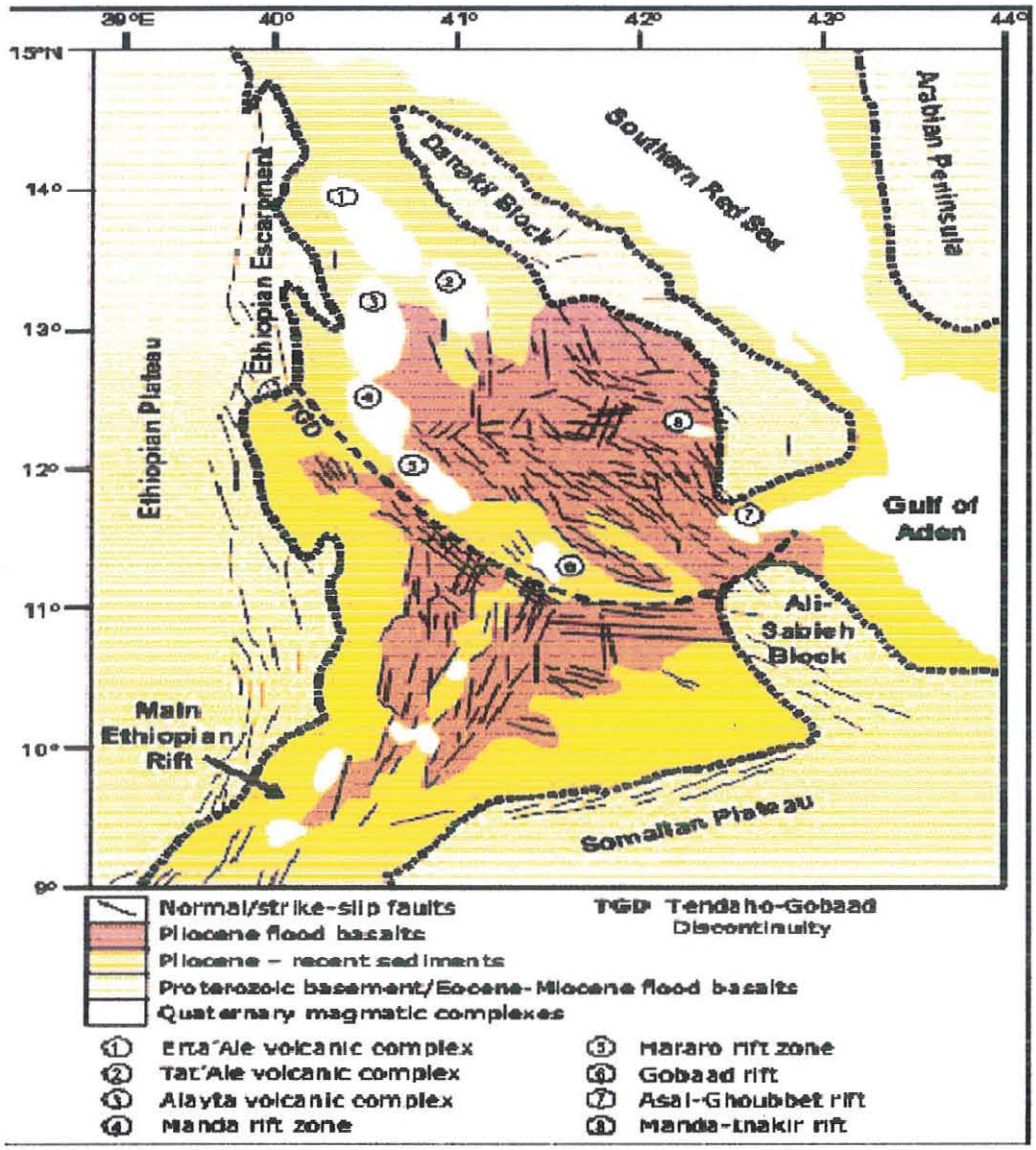

Figure 2.1 Geological map of the Main Ethiopia Rift

CHAPTER THREE

3. GRAVITY METHOD

3.1. Introduction

If we let a body, initially at rest fall freely on the earth it acquires a velocity of about 9.80 m/s in the vertical direction at the end of one second. After a further period of the 1sec the velocity is 9.80m/s + 9.8 0m/s =19.60m/sec ,and So on .The increase, during each second of fall of 9.80m/see in the vertical velocity of a freely falling body is called the gravitational acceleration or simply the gravity.

Gravity prospecting involves the measurement of variations in the gravitational field of the earth. The observations are normally made within a few feet of the earth surface or on ship; airborne tests and underground surveys have also been carried out occasionally. In gravity measurements, the quantity actually observed is not the earth's true gravitational attraction but its variation from one point to another, usually at positions along the earth's surface which are close together. Such lateral differences can be measured with a much greater degree of precision than the total gravitational field, and field instruments are designed to measure differences in gravity rather than its actual magnitude.

The variations in gravity observed through such measurements depend only upon lateral changes in the density of earth materials in the vicinity of the measuring point. In other words, the variations in gravity anomalies are indicative of subsurface variations in the density of rocks.

3.2. The reasons of measuring earth's gravity

The five main purpose of measuring earth's gravity are:

1. For geodetic application.
2. To know underground mass distribution.
3. To estimate the elasticity of the earth.
4. To observe the secular variation of gravity field due to internal earth process.

5. To standardize some physical and chemical constants.

3.3. Fundamentals of Gravity Method

The expression of gravitational attraction in a form most useful for application to exploration requires an understanding of the basic physical concepts relating force, acceleration and potential. To do with these basic principles first we should have to assume that the simplified earth model , that is the earth is:-

- Spherical in shape
- Has no density variation within
- Doesn't rotate
- The Only celestial body in the universe

3.3.1. Gravitational Force:-

Newton's law expressing the force of mutual attraction between two mass particle interms of their mass and separation. This law states that the force between two masses is directly proportional to the product of the two masses; m_1 and m_2 and inversely proportional to the square of the distance between the centers of masses. This force is given by the equation.

$$F = -\gamma \frac{m_1 m_2}{r^2} \quad \text{...} \; 1$$

Where: - γ is known as the universal gravitational constant depends on the system of units employed. In the centimeter-gram-second (cgs) system, the value of γ is $6.670 \times 10^{-8} cm^3/gms^2$

3.3.2. Gravitational Acceleration:-

The acceleration of m_2 due to the presence of m_1 can be found by dividing F by m_2.In particular, if m_1 is the mass of the earth; M_e, the acceleration of the mass m_2 at the surface of the earth is

$$g = \frac{F}{m_2} = -\gamma \frac{M_e}{R_e^{\,2}} \quad \ldots\ldots 2$$

R_e being the radius of the earth. This acceleration, which we call the acceleration of gravity. The numerical value at the earth's surface is about 980cm/sec^2. In honor of Galileo, the unit of acceleration of gravity 1cm/sec^2, is called gal.

The acceleration, being the force acting on a unit mass, is the conventional quantity used to measure the gravitational field acting at any point. All masses located at the same position in the field are subject to the same gravitational acceleration.

3.3.3. Gravitational potential:-

As the intensity of gravitational, magnetic, or electric fields depend only on positions, the analysis of such fields can often be simplified by using the concept of potential. Gravitational fields are conservative, that is to say, the work done to move a mass in a gravitational field is independent of the path traversed and depends only on the end points. In fact if the mass is eventually returned to its original position the net energy expenditure is zero, regardless of the path followed.

The force giving rise to a conservative field may be derived from a scalar potential function

$$\nabla U(r) = F(r)/m_2 = g(r) \quad \ldots\ldots 3$$

Alternatively, we can solve this equation for the gravity potential in the form

$$U(r) = \int_{\infty}^{R} g(r).dr = -\gamma \int_{\infty}^{R} \frac{dr}{r^2} = \gamma \frac{M}{R} \quad \ldots\ldots 4$$

Which is a statement of the work done in moving unit mass from a very distance point (infinity) by any path at all to a point distant R from the center of gravity of M.

Any surface along which the potential is constant is referred to as an equipotential surface.

3.3.3.1. Two Dimensional Potential

Consider the attraction of an irregular laminar body (part of a two-dimensional sheet) in the XZ plane at an external point P (Fig.3.1). We must first determine the X (horizontal) and Z (vertical) components of acceleration at P associated with this attraction.

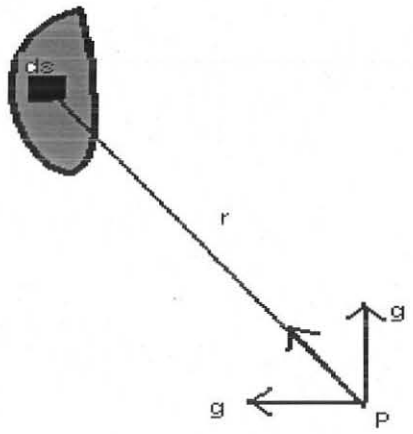

Figure3.1 determining gravitational acceleration of irregular two dimensional sheet. ΔS is elements of area.

If the mass is very long in the Y- direction and has a uniform cross-section of arbitrary shape in the XZ- plane. Then the equation becomes.

$$U = 2\gamma\sigma \int_x \int_y \log(\frac{1}{r}) dxdy \quad \ldots\ldots 5$$

The gravity effect for the two dimensional body is

$$g_z = \frac{\partial U}{\partial Z} = -2\gamma\sigma \int_x \int_z \frac{Z}{r^2} dxdz \quad \ldots\ldots 6$$

Where $r = (x^2 + y^2)^{1/2}$

Note that, if the density (σ) is a function of the coordinates as well, the potential can be calculated only for a few simple shapes. These are the basic equations for calculating the gravity effects of bodies of uniform density. The use of the above equations make it possible to obtain closed analytical expressions for the gravity effects of bodies of regular shape such as sphere, cylinder, horizontal slab etc. of the most widely used is the gravity formula for an infinitely extended horizontal slab that has been employed in computation of Bouquet slab given by

$$g_B = 2\pi.\gamma.\sigma.Z \quad \ldots\ldots\ldots\ldots\ldots\ldots\ldots\ldots\ldots\ldots\ldots\ldots\ldots\ldots\ldots\ldots\ldots\ldots\ldots\ldots 7$$

Where σ the density and Z is the thickness of the slab.

In gravity work, computations are often simplified using the scalar potential; U, instead of the vector g. The first derivative of U in any direction gives the component of gravity in that direction, as a result of a potential field approach provides computation flexibility.

3.3.3.2. Three Dimensional Potential

Considering a three dimensional mass of arbitrary shape as shown bellow, the potential and the acceleration of gravity at appoint some distance away can be calculated by dividing the mass in to small elements.

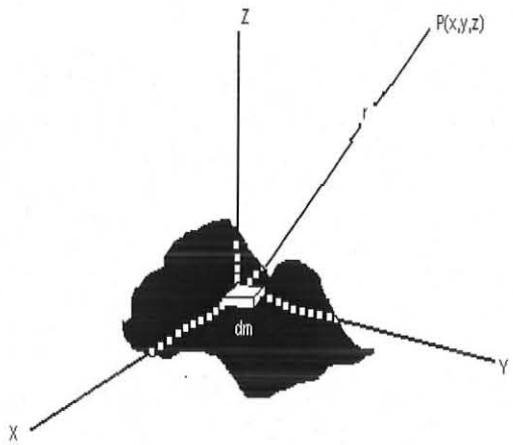

Figure3.2 Potential of three dimensional mass

And integrating it to get the total effect. Cleanly it is easier to use the potential, if the problem can be solved at all. The potential due to an element of mass dm at a distance r from p is

$$dU = \gamma \frac{dm}{r} = \gamma \frac{dxdydz}{r} \quad \ldots\ldots 8$$

Where σ is the density and

$r = (x^2 + y^2 + z^2)^{1/2}$

Then the potential of the total mass m will be

$$U = \gamma\sigma \int_X \int_Y \int_Z \frac{1}{2} dxdydz \quad \ldots\ldots 9$$

For cylindrical coordinates: - the above expression

$$U = \gamma\sigma \int_r \int_\phi \int_z drd\phi dz \quad \ldots\ldots 10$$

Since $dxdydz = rdrd\phi dz$

For Spherical Coordinates: -

$$U = \gamma\sigma \int_r \int_\phi \int_\theta r \sin\theta . drd\phi d\theta \quad \ldots\ldots 11$$

Since $dxdydz = r^2 \sin\theta . drd\phi d\theta$

The acceleration in the direction of the Z-axis is given by

$$g_z = \frac{\partial U}{\partial Z} = -\gamma\sigma \int_X \int_Y \int_Z \frac{Z}{r^3} dxdydz \quad \ldots\ldots 12$$

For cylindrical coordinate systems the acceleration in the Z- axis is given by

$$g_z = -\gamma\sigma \int_r \int_\phi \int_z \frac{Z}{r^2} drd\phi dz \quad \ldots\ldots 13$$

For spherical coordinate systems is given as

$$g_z = -\sigma\gamma \int_r \int_\phi \int_\theta \frac{Z}{r} \sin\theta . drd\phi d\theta \quad \ldots\ldots 14$$

$$g_z = -\gamma\sigma \int_r \int_\phi \int_\theta \sin\theta . \cos\theta . drd\phi d\theta \quad \ldots\ldots 15$$

3.4. Equations of potential fields

The divergence theorem (Gauss' theorem) states that the integral of the divergence of a vector field over a region of space is equivalent to the integral of the out word normal component of the field over the surface enclosing the region.

Mathematically, we have

$$\int_V \nabla.g dv = \int_S g_n ds \quad \text{..... 16}$$

If there is a particle of mass m within the volume and in particular, if we consider it to be at the center of a spherical surface of radius r, the right-hand side of the gauss theorem equation is

$$\int_S g_n ds = -\left(\frac{\gamma.m}{r^2}\right)\left(4\pi r^2\right) = -4\pi\gamma.m \quad \text{.....17}$$

And, if the surface encloses several particles of total mass M, we can write as.

$$\int_V \nabla.g dv = \int_S g_n ds = -4\pi\gamma.M \quad \text{.....18}$$

If this volume V is made very small enclosing a point in the region, we may move the integral sign to give.

$$\nabla.g = -4\pi\gamma\sigma \quad \text{.....19}$$

Where σ is the density at that point. Then it will be

$$\nabla^2 U = -4\pi\gamma\sigma \quad \text{.....20}$$

This is *Poisson's equation*

If there is no attracting matter contained within this volume, the integrals are zero and.

$$\nabla.g = 0 \quad \text{.....21}$$

But the gravitational force is the gradient of scalar potential, so that

$$\nabla.g = \nabla.\nabla U = \nabla^2 U = 0 \quad \text{.....22}$$

Therefore; we see that the gravity potential satisfies Laplace's equation in a free space and Poisson's equation in a region congaing attracting material.

3.4. Derivatives of the potential

3.4.1. Vertical gravity component:-

It is often simpler to obtain gravity effects by employing the potential first and then taking the derivative. Other quantities useful in gravity analyses may also be obtained by differentiating the potential in a variety of ways.

Vertical gravity g_z is the derivative of potential in the direction of the vertical axis. This is the quantity measured by gravimeters. If we calculate the first vertical derivative of g_z we can find that

$$\frac{\partial g_z}{\partial z} = \frac{\partial^2 U}{\partial Z^2} = -\gamma\sigma \iiint \left(\frac{1}{r^3} - \frac{3z^3}{r^5} \right) dxdydz \quad \text{.....23}$$

For two-dimensional case.

$$\frac{\partial g_z}{\partial z} = 2\gamma\sigma \iint \left(\frac{2z^2 - r^2}{r^4} \right) dxdz \quad \text{.....24}$$

The second derivatives for the same equations are, for the three-dimensional body.

$$\frac{\partial^2 g_z}{\partial z^2} = \frac{\partial^3 U}{\partial z^3} = -3\gamma\sigma \iiint \left(\frac{5z^3}{r^7} - \frac{3z}{r^5} \right) dxdydz \quad \text{.....25}$$

For two dimensional.

$$\frac{\partial^2 g_z}{\partial z^2} = 4\gamma\sigma \iint \left(\frac{3z}{r^4} - \frac{4z^3}{r^6} \right) dxdz \quad \text{..... 26}$$

Although the first derivative is not much used at present, attempts have been made to measure vertical gradient in one type of airborne instrument, as well as much earlier with a modified torsion balance.

The second vertical derivative of g_z has been employed considerably in gravity interpretation work for upward and downward continuation and for the enhancement of small anomalies at the expense of large scale effects. Obviously both derivatives tend to

magnify near-surface feature and discriminate between them, by increasing the power of the linear dimension in the denominator.

3.4.2. Horizontal gravity gradient (HGG)

By taking the derivative of g_z along the x- or y- axis, we obtain the components of the horizontal gradient of gravity, using subscripts to denote differentiation; we get for the y- component of the three-dimensional body.

$$U_{XZ} = \frac{\partial^2 U}{\partial x \partial z} = 3\gamma\sigma \iiint_{x\ y\ z} \frac{xz}{r^5} dxdydz \quad \text{.....27}$$

For two dimensional body of the y-component is

$$U_{XZ} = \frac{\partial^2 U}{\partial x \partial z} = 4\gamma\sigma \iint_{x\ z} \frac{xz}{r^4} dxdz \quad \text{.....28}$$

The horizontal gradient can be obtained by torsion balance measurement. Otherwise it can be determined from gravity profiles or contours, as the slope or rate of change of g_z with horizontal displacement. This is a very significant parameter in gravity interpretation, since the sharpness of a gravity profile is an indication of the depth of the anomalous mass.

3.5. The earth's gravitational field

As all gravity measurements made in exploration work show only differences in gravity from one place to another, the attraction of the earth itself is significant only insofar as it varies laterally over the earth's surface. Such variation must be taken in to account in evaluating the gravity effect of buried bodies having geological or exploration significance.

If the earth were made up of homogeneous spherical shells and did not rotate, the attraction at the surface of the earth would be the same every where and it would not

affect the reading of gravity meters, which measure only differences in acceleration between one place and another.

To predict the gravitational field of the earth precisely at any point, we must know its shape and density distribution with the greatest possible accuracy. Because of its rotation, the earth is not actually spherical. Its shape can be approximated as an oblate spheroid (a surface generated by revolving an ellipse around its minor axis) with an eccentricity of 1/297. Both its departure from sphericity and its rotation (because of associated centrifugal forces) cause the earth's gravitational acceleration to have a maximum value at the poles and a minimum at the equator.

A good overall fit to the observed relation between gravity and latitude, based on measurements made in all parts of the earth, it obtained by using the International Formula, widely accepted as the standard for theoretical prediction of gravity over a laterally homogeneous spheroid earth.

This formula, which gives gravity as a function of the angle of latitude Ø, is

$$g = 978.049\left(1 + 0.0052884\sin^2\phi - 0.0000059\sin^2 2\phi\right) \quad \ldots\ldots 29$$

The International Formula is one of several relations proposed for predicting the earth's gravitational force at the surface on a global scale. Others are similar in form but use slightly different constants. The actual difference in gravity between the equator and pole is about 5.3 gals, or 5300mgal, although a theoretical calculation based only on the earth's rotational characteristics and the difference in distance from the earth's center at the two positions would lead one to expect about twice the contrast that is actually observed between pole and equator. International formula is based on the assumption that the sea-level surface is smooth.

3.6. The Reference Spheroid, Geoid and Ellipsoid

3.6.1. The Reference Spheroid:-

The surface of the earth is defined as a mathematical figure in terms of the gravity value at all surface points. This mathematical figure is known as the reference spheroid. It is related to the mean sea level surface with excess land masses removed and ocean deeps filled. The formula, adopted by the International Association of Geodesy in 1967, gives the value of g at any point on this spheroid as

$$g = g_0\left(1 + \alpha \sin^2 \phi + \beta \sin^2 2\phi\right) \quad \ldots\ldots 30$$

Where, g_0 = equatorial gravity

= 977.0318gals

ϕ = Latitude

α = 0.0053024 and

β = -0.0000058

Thus, the above equation is quite accurate enough to be used for calculating the variation of gravity with latitude.

3.6.2. The Geoid:-

The gravity relation in eq.29 is a very crude approximation. It assumes that there are no undulations in the earth's surface. Whereas infact we have mean continental elevations of about 500 meters and maximum land elevation and ocean depressions of the order $\pm$ 9000 meters, all referred to sea level obviously the true sea level is influenced by these variations and the surveyor must take them in to account when measuring elevations.

The geodesist defines practical mean sea level (equipotential) surface for making these measurements. It is known as the geoid and is defined as average sea level over the ocean and over the surface of sea water which would lie in cannels, say cut through the land masses.

Clearly the geoid and reference spheroid surfaces do not in fact, never could coincide at all points, since the geoid is warped upward under the continental masses due to attracting material above and downward over the ocean basing.

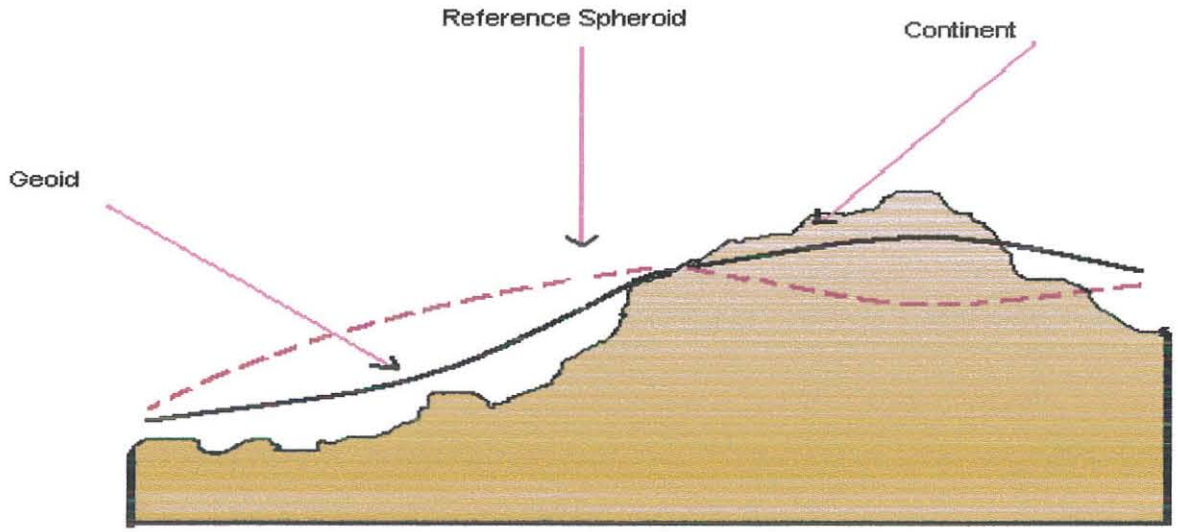

Fig.3.3 Comparison of spheroid and geoid

CHAPTER-FOUR

4. GRAVITY DATA AND REDUCTIONS

4.1. Gravity Data

Gravity data is collected through gravity surveying, conducted by making gravity-meter readings at many locations in an area of interest other measurements and observations, other than gravity, must also be made to describe the position of each observation site. Especially important are latitude and elevation because these values enter directly in to the computation of gravity anomalies further more we must note the time when each reading is made so that corrections for gravimeter drift can be determined.

The object of a survey is to measure the value of gravity of at the observation sites where changes in gravity Δf between these places and a conveniently located reference site called a base station, where gravity has already been determined. The base station should be one of the sites in the 1971 International Gravity Standardization Net (IGSN71) if none of these sites are close to the survey area, it may be necessary to determine the reference value of gravity, of g at a mane conveniently located base station using gravimeter measurements adjusted to the IGSN71.

We shall now consider the techniques by which gravity data are obtained in land surveys and converted in to a form suitable for interpretation. The development of the equipment and techniques used for making gravity observations in the field has refined a rare combination of engineering skill and operational efficiency. The instrument have been designed for ruggedness so they can operate reliably under difficult field conditions, and the procedures used in obtaining data with them have been designed for maximizing the speed with which traverses can be covered.

The placement of stations in gravity survey depends on two factors:-

1. Feasibility of access and

2. The spacing pattern necessary to detail the features which the survey was designed to locate and map.

Access depends on the nature of the terrain and the distribution of roads or other thorough fares (such as streams) through the area being surveyed in most surveys, the objectives can be achieved if gravity stations are confined to existing roads to waterways.

The pattern of the stations is generally designed so that they will come as close to forming a rectangular grid as access conditions allow. The spacing within the grid is governed by the depth and lateral extent of the geological features being sought.

The methods of surveying and the cost involved vary greatly, depending on the ease of transportation on the scale quality of existing maps and level nets. The degree of necessary precision is established by the sensitivity of observed gravity to elevation and latitude.

4.2. Reductions of Gravity Data

In order to be most useful in prospecting gravity data as obtained in the field must be commented for elevation, the influence of nearly topography, and latitude, hence must be corrected for variations in latitude, elevation and topography to reduce them to the values they would have on some datum equipotential surface, such as the geoid, or a surface every where parallel to it. Two additional corrections may occasionally be required these are due to earth tides and the effect of isostasy.

4.2.1. Elevation Correction

Let us assume that gravity observations are made at two stations s_1 and s_2 each located on tertian that is entirely flat except for the cliff midway between them as shown in fig.4.3. The elevation g s_1 above sea level is h_1, and that of s_2 is h_2.

The stations are so far a part that each is effectively on a horizontal surface of infinite extent. Because the elevations are different, however, there would be a difference in the two gravity readings which must be removed to avoid an indication of a subsurface structure that is not really there.

A datum plane is introduced with an elevation above sea level of d, all material above the datum plane being effectively "removed" so that the readings of both instruments are adjusted to be the same as it they were on the datum surface.

The adjustment actually consists of two parts

1. The free air correction
2. The Bouguer correction

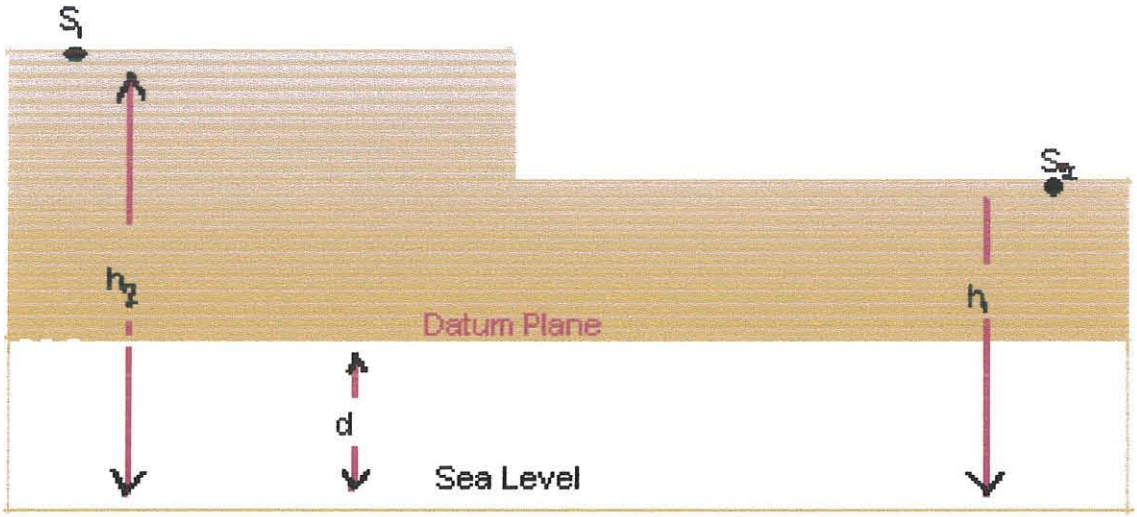

Fig.4.1 Elevation correction

4.2.1.1. The Free Air Correction

Which accounts for the fact that each station is a different distance from the earth's center than the datum plane and it is based on the fact that the attraction of the earth as a whole can be considered to be the same as if it's mass were concentrated at its center.

If the elevation of a gravity meter is charged, its distance from the center of the earth changes by the same amount.

If the radius of the earth (at sea level) is R the height above sea level is h, and the value of gravity at sea level is go, then of the gravity at h, can be expressed as

$$g = g_0 \frac{R^2}{(R+h)^2} = g_0 \frac{1}{1+2\frac{h}{R}+\frac{h^2}{R^2}} \quad \text{.....31}$$

$$g = g_0 \frac{1}{1+2h/R} \quad \text{As} \quad \frac{h^2}{R^2} << 2\frac{h}{R} \quad \text{.....32}$$

Using the first term of the binomial expansion

$$g = g_0\left(1-2\frac{h}{R}\right) \quad \text{.....33}$$

One obtains

$$g - g_0 = \delta g_f \approx -2\frac{hg_0}{R} \quad \text{Or} \quad \delta g_f = -0.3086h \quad \text{.....34}$$

Where $g_o = 978000mGal$

$R = 6.378 \times 10^6 m$

This effect will be independent of whether or not there is any rock material between the sea level datum and the station at elevation h. It is referred to for this reason as the free air effect and the portion of the elevation correction which compensates for it is referred to as the free air correction.

If h is positive, i.e. the elevation is above sea level, the effect is to lower the earth's attraction to compensate for this lowering the free air correction must be added.

4.2.1.2. Bouguer Correction

This removes the effect of a presumed infinite slab of material between the horizontal plane of each station and the datum. If the station is located on an extended horizontal surface having an elevation h above sea level, one must also correct for the attraction of the slab of material

elevation of the station. If the material introits slab has a density of g, this attraction will be

$$\delta g_B = 2\pi\rho h$$
$$Or \qquad \ldots\ldots\ldots\ldots\ldots\ldots\ldots\ldots\ldots\ldots \qquad 35$$
$$\delta g_B = 0.04193\rho h$$

So it is subtracted from the observed reading the Bouguer correction is applied in the opposite sense to free air, that is, it is subtracted when the station is above the datum plane and vice – versa.

4.2.2. Terrain Correction

This correction allows for surface irregularities in the vicinity of the station, that is hill rising above the gravity station and valleys (or lack of material) below it from fig.3.5 it is obvious that both of these tog graphic undulations affect the gravity measurement in the same sense, reducing the readings because of upward attraction (hills) or lack of downward attraction (valleys). Hence the terrain correction is always added to the station reading.

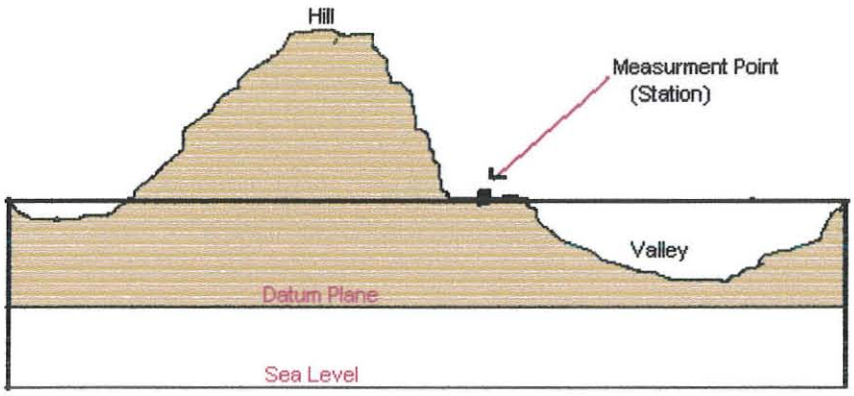

Figure 4.2 Terrain correction removes effect of hill by adding its up-ward attraction at station and compensates for valley by adding attraction it would exert at station is filled in result is to flatten all topography to level of station.

There are several graphical methods for calculating terrain corrections. All of them require a good topographical map of the area (so fat contours or smaller) extending if possible considerably beyond the survey grid (within which, of course, the elevations are known more precisely). The usual procedure is to divide the area into compartments and compare the average elevation within each compartment with the station elevation. This is best done by out ling the compartments on a transparent sheet which overlies the topographic map.

The most commonly used template is a set of concentric circles and radial lines, making sectors whose areas increase with distance from the centre the gravity effect of a single sector can be calculated from the formula.

$$\delta g_f = \gamma\sigma\theta\{(r_0 - r_i) + \sqrt{(r_i^2 + z^2)} - \sqrt{(r_o^2 + z^2)}\} \quad \ldots\ldots\ldots\ldots\ldots\ldots 36$$

Where θ = sector angle (radians)

$Z = |e_s - e_a|$

- e_s =station elevation
- e_a =average elevation in sector

r_o = Outer sector radians

r_i = inner sector radians

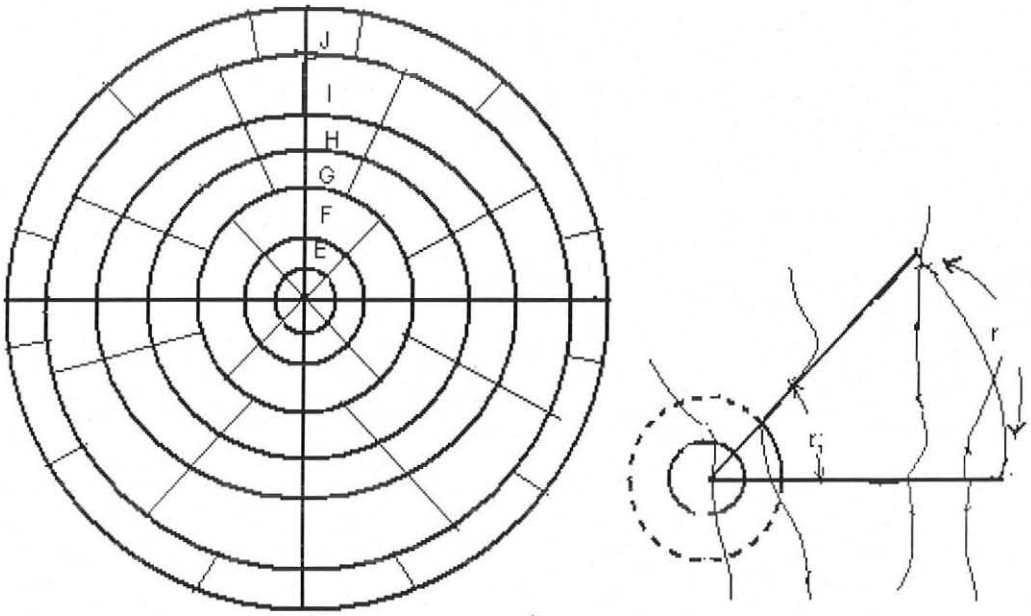

Figure4.3 Use of terrain chart with topographic map (a) terrain chart overly topographic map (b) Enlarged view of a single zone.

The terrain correction is the sum of all the sectors. Therefore, if we have n number of sectors, the total terrain correction will be

$$\delta g_T = \eta.\sigma.g_t(r,\theta) \quad \ldots\ldots 37$$

The terrain correction is positive regardless of whether the local topography consists of a mountain or a valley region. As a result the terrain correction is always added to the station reading the terrain reduced gravity is given by

$$\Delta g = g_{Obe} + \delta g_f - \delta g_B + \delta g_T \quad \ldots\ldots 38$$

4.2.3. Drift Correction

Gravimeter reading changes (drift) with time as a result of elastic greening in the springs the instrumental drift can be determined by repeating measurement at the base station at different times of the day (1-2hr) and the difference between successive measurement at the same static at different time are platted to produce a drift cure.

The observed gravity values from other stations can be corrected by subtracting the amount of drift from g_{Obs}.

4.2.4. Latitude Correction

The international formula for the variation with latitude ∅ of normal gravity g, in gals, on the international Ellipsoid is

$$g = 978.049\left(1 + 0.0052884\sin^2\phi - 0.0000059\sin^2 2\phi\right) \quad \ldots\ldots 39$$

Let us differentiate this equation with respect to ∅, converting the angular differential to one terms of distance in this way we obtain the following expression for w, the rate of change of gravity with north-south displacement as a function of latitude

$\omega = 1.307 Sin2\phi.mgal/mile$

The maximum value occurs at latitude 45^0 where the correction amounts to 0.01mgal/40ft. It is obviously zero at the equator and poles. The correction is linear over north south distances of about one mile. For larger surveys it is necessary to take account of the changes in Ø. Since gravity increases w3ith latitude (either north or south) the correction is added as we move towards the equator.

4.2.5. Tide Correction

The normal value of gravity at any point will vary cyclically during the course of the day by as much as 0.3mgal because of the tidal attraction of the sun and the moon. In a high precision survey this much variation might well be a significant source of error in the relative gravity between two points at which measurements are made at different times. There are two methods of correcting for the tidal effect one is to construct daily charts of the tidal variation in gravity with time from readings on a stationary instrument and to correct all readings in the field by means of such charts. The more usual method is for the observer to return to the base station so often that earth tide effect will be fully incorporated in to the instrumental drift curve.

4.3. Gravity Anomaly

Gravity anomalies (Free-air and Bouguer) are geophysical tools up on which effects of geology on the earth's gravity field can be detected. In order to get the designed anomaly that is caused by geologic structure, we have to correct the measured gravity value, from the corrections that we have mentioned before.

Considering that the above corrections have accurately accounted for the variations in gravitational acceleration they were intended to account for any remaining variations in the gravitational acceleration associated with the terrain corrected Bouguer gravity anomaly can now be assumed to be caused by geologic structures.

4.3.1. Simple Bouguer Anomaly

The simple Bouguer gravity anomaly corrects for the free air gravity anomaly for the material slab exists between the station elevation and the geoid surface however, terrine effect is not taken care off here. The simple Bouguer anomaly is determined from the given formula

$$\Delta g_{SB} = g + \delta g_F - 0.04198088\rho.h - g_{\phi(1971)} \ldots\ldots\ldots\ldots\ldots\ldots\ldots 40$$

Where: - δg_F = Free air correction

ρ = Average subsurface density

h= station elevation with reference to genocidal surface

g_ϕ = Theoretical calculated value

4.3.2. Complete Bouguer Anomaly

The complete Bouguer Anomaly corrects the Simple Bouguer gravity anomaly for topographic irregularities of the earth in the vicinity of a gravity station. To mansion this anomaly takes account the free-air. Bouguer slab and Terrain corrections.

If the earth crust had no lateral variation in density, asset of measured gravity values taken care of the aforementioned reductions would be identical of this junctures differences in the properly corrected values constitute a gravity anomaly. Known as the complete or terrain corrected Bouguer anomaly, the result of lateral variations in sub surface densities.

The terrain corrected Bouguer anomaly for the some station is obtained by:

$$\Delta g_{CB}(g,h,\phi,\rho,) = \Delta g_{SB}(g,h,\phi,\rho) + \delta g_T \ldots\ldots\ldots\ldots\ldots\ldots 41$$

Finally the above equation is given a

$$\Delta g_{CB}(g,h,\phi,\rho) = g_{Obs} + \delta g_F(h,\phi) - \delta g_B(\rho,h) + \delta g_T - g_\phi \ldots 42$$

CHAPTER-FIVE

5. GRAVITY DATA PROCESSING AND QUALITATIVE INTERPRETATION

5.1. The Data:-

These data distribution consists of 171 gravity measurement station points and all station were tied to IGSN 1971 (International Gravity Standardization Net 1971, Morlli et.al., 1971). The entire gravity data set was reduced by making fundamental corrections, including terrain, free-air, drift and latitude correction.

The free-air and Bouguer gravity anomalies were calculated using the Geodetic Reference system of 1930 (GRS 30) and the reduction taken place to make it to sealevel using a uniform crustal density. Then, after the data can be analyzed using two-dimensional smoothing of the noise created through extrapolation and then extracting one-dimensioned profiles from the smoothed map.

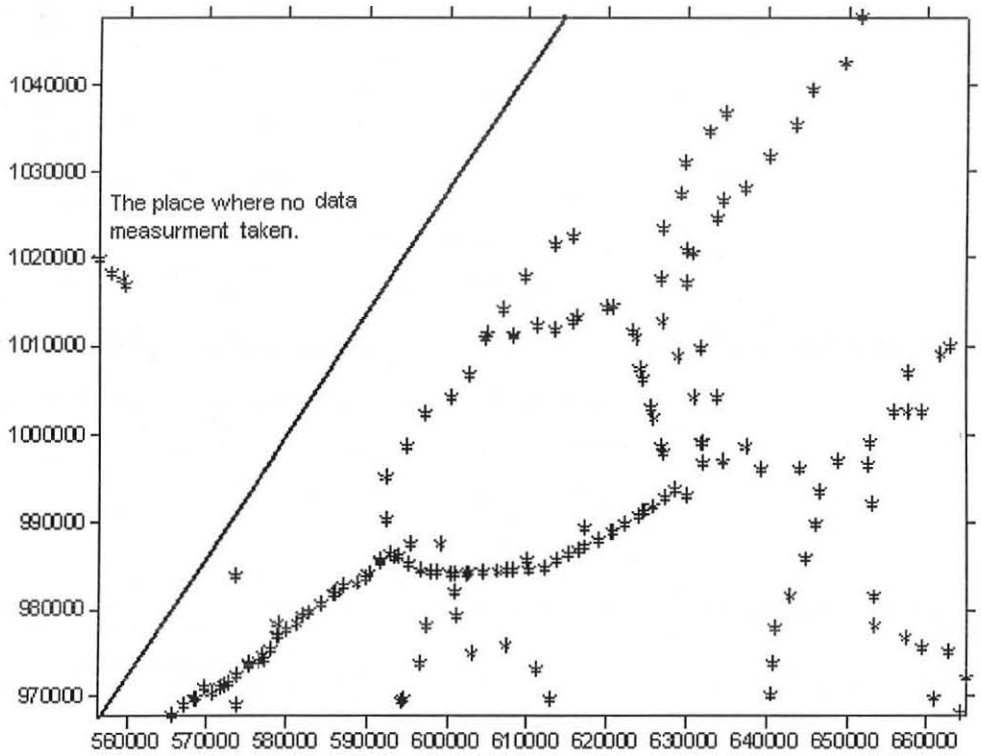

Figure5.1 Data measurement station points

5.2. Gravity Data Analysis and Qualitative Interpretation

5.2.1. Bouguer Anomaly Map

The Bouguer Anomaly Map in fig.5.2 was equipped based on software so called sulfer8, using a geostatic gridding method which is known as **krigning**. The map which is shown below indicates an overview of the topographic feature and underling the crustal structure of the study area.

From the map shown bellow the highest minimum and its relative minimum gravity anomaly is observed over the western plateau of the study area. While; the other minimum value is over the lower corner of S-E trend of the Bouguer anomaly map. This low anomaly over the map may be related with the crustal thicken of the western plateau and the other low value which may be associated with the Somalian plateau. Where as the intermediate lower anomalies observed over NNE-SSE trend .While, the maximum gravity anomaly found over N-E of the Bouguer anomaly and it is probably related to the crustal thinning.

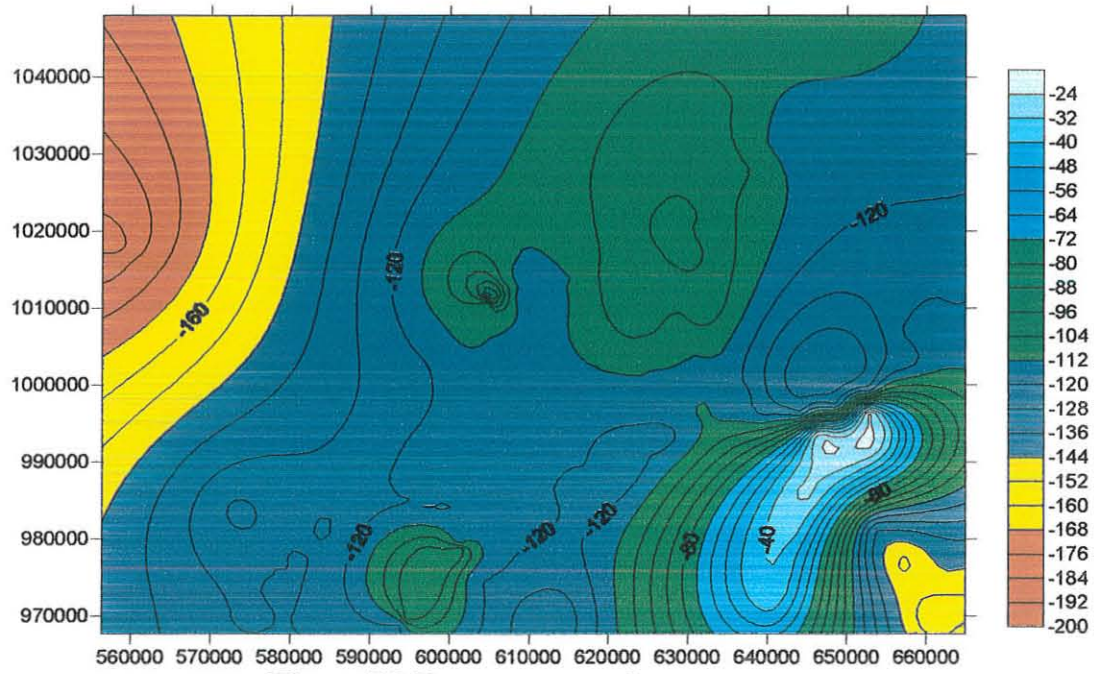

Figure 5.2 Bouguer anomaly map.

5.2.2. Regional Residual Separation

Most gravity or maps that emerge after Bouguer reduction represents the superposition of anomalies of different wavelengths, that are caused by different subsurface of different sizes located in different depths. Small near surface bodies generates very sharp high frequency anomalies and deep or large size bodies cause long wavelength effects. Depending on the need at hand it might be necessary to focus either on the high or low frequency anomalies. The high frequency anomalies are called **the residual anomalies** and the long wavelength effects are called **the regional** or **the trend effect.**

The separation of the trend from the residual anomaly is an interpretation technique that can be carried out using different approaches. The anomaly maps given bellow were separated using a Polynomial fitting technique of different order of degree.

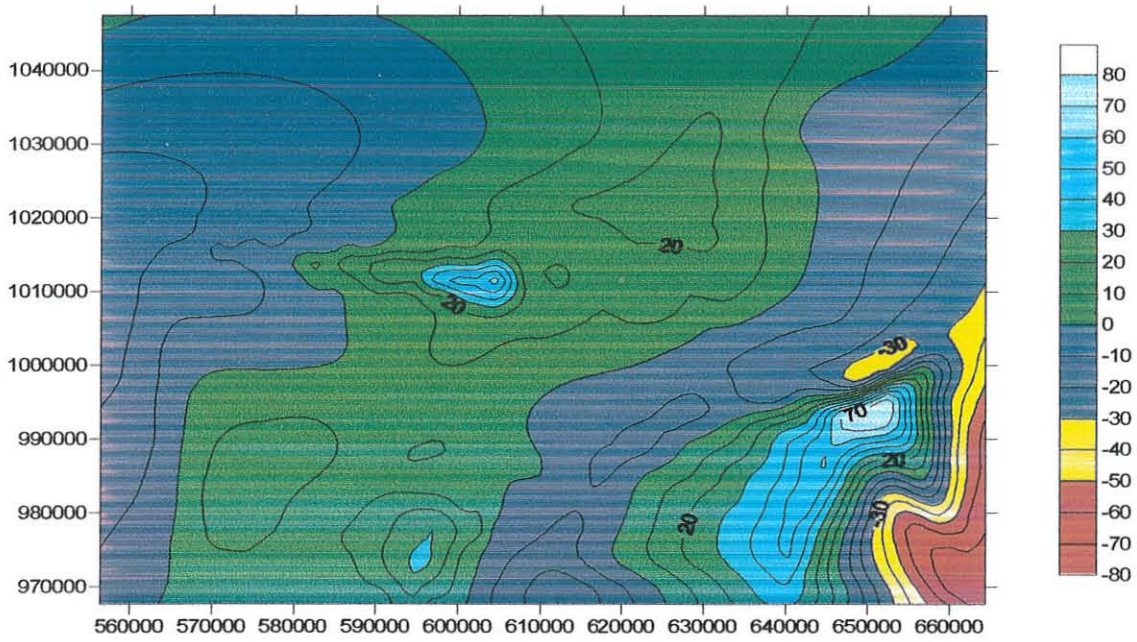

Figure 5.3.Residual Bouguer Anomaly Using Polynomial of Degree 1

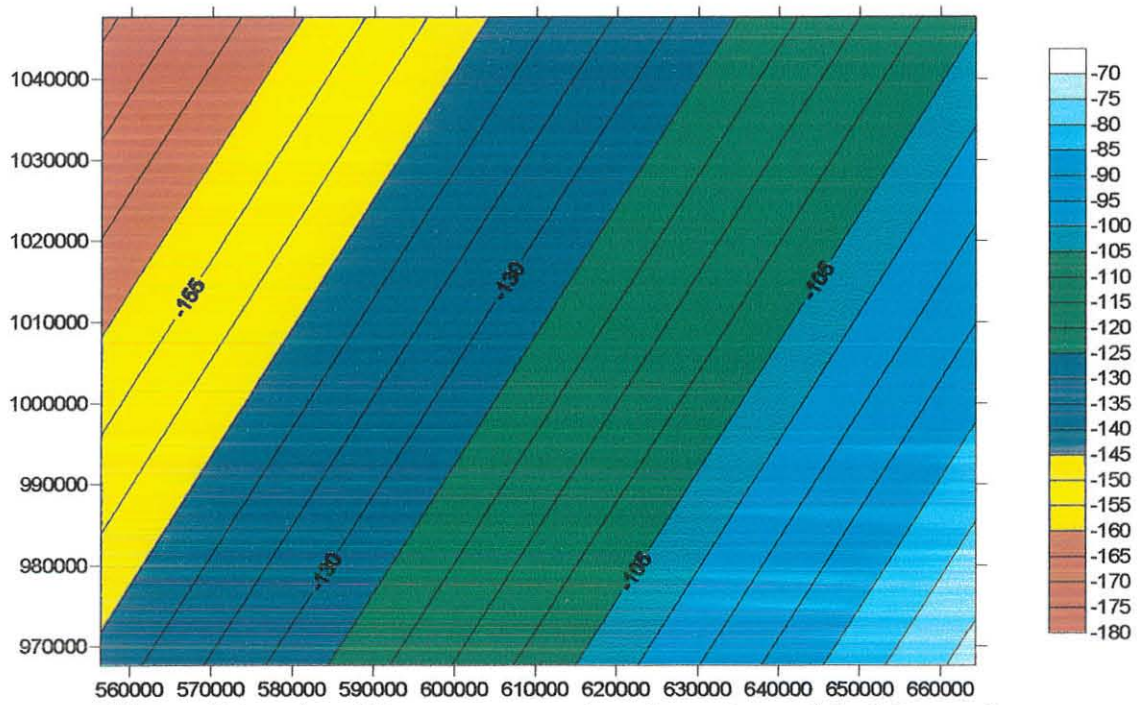

Figure 5.4 regional Bouguer anomaly using polynomial of degree 1.

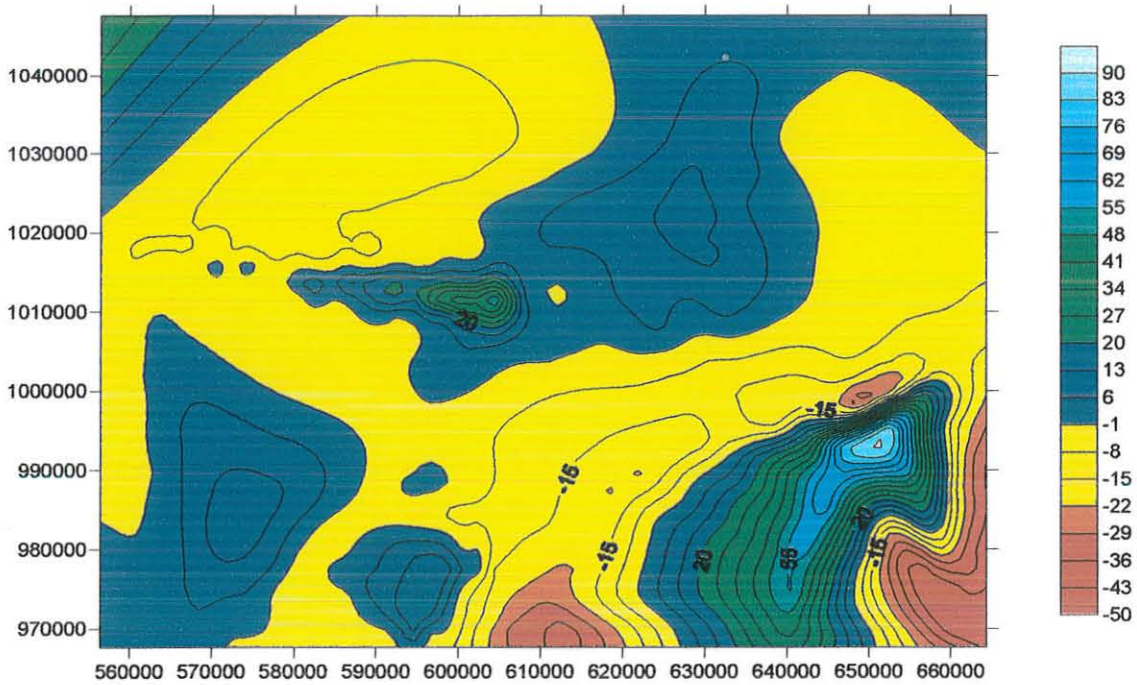

Figure 5.5 residual Bouguer anomaly using polynomial of Degree 2.

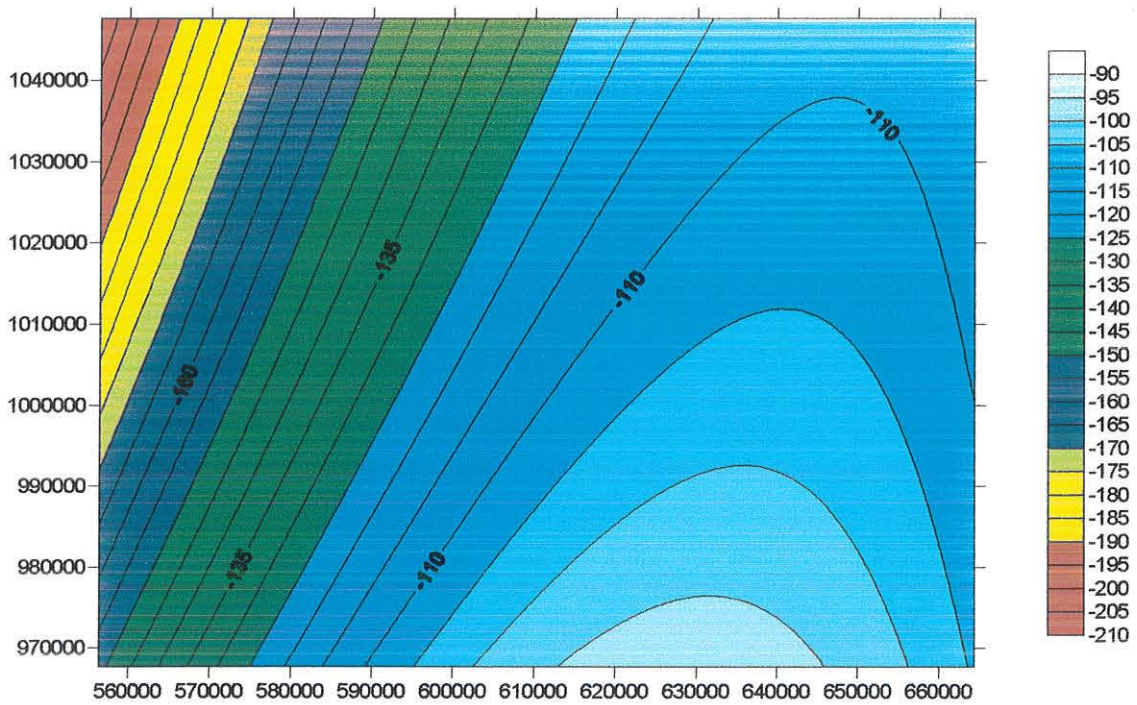

Figure 5.6 regional Bouguer anomaly Using polynomial of degree 2.

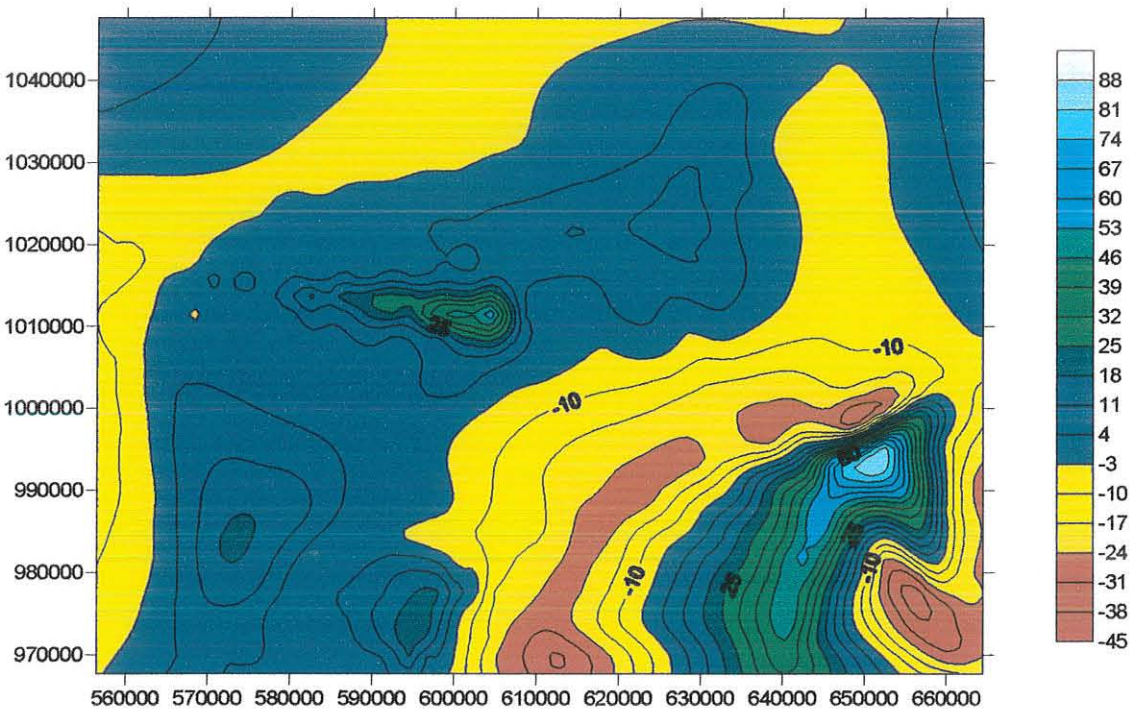

Figure 5.7 residual Bouguer anomaly using polynomial of degree 3.

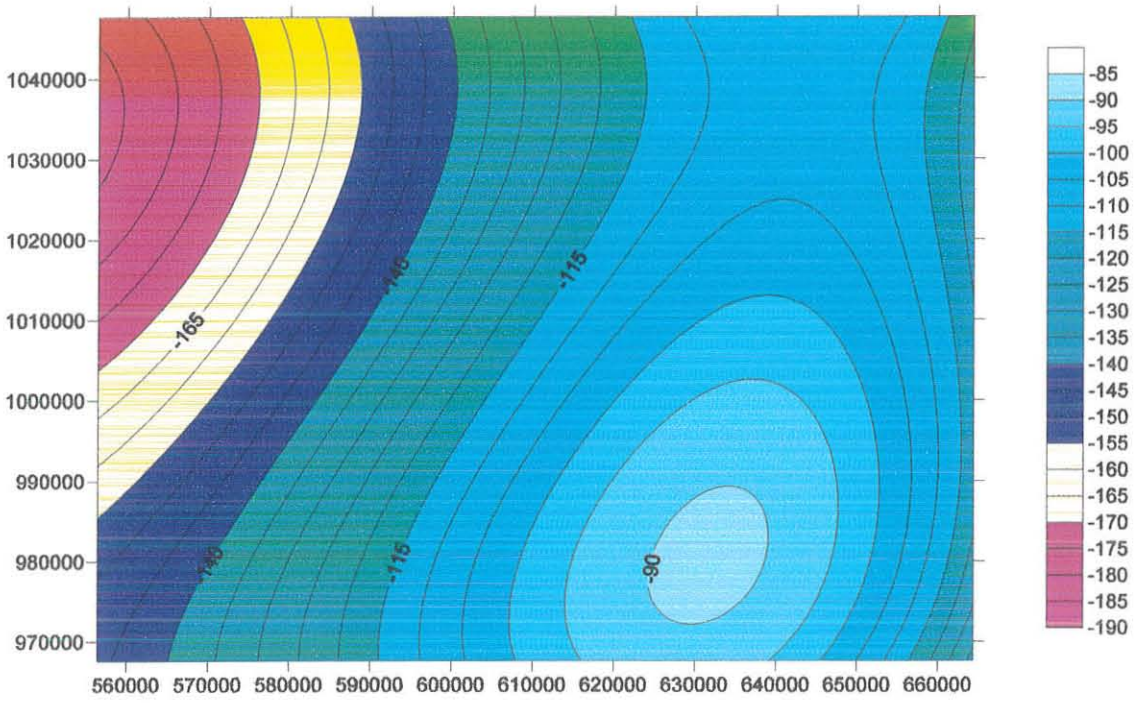

Figure 5.8 regional Bouguer anomaly using polynomial of degree 3.

5.2.3. Residual Gravity Anomaly Map.

The map which is show in **fig 5.5** has contour internal of 7mgal and scale value varies in between -50 and 97mgal and its highest (positive) value is located at the lower corner of S-E part of the map, where condensed gradient observed and It may be caused by a plug type of structure or intrusion and it probably would be found on the upper crust with considerable high positive density contrast. While the other highest positive anomaly observed in the central region of the residual anomaly, it is also some what related the geologic structure that is observed at the lower corner of S-E part of the map. The residual anomaly also in counters the most low (negative) anomaly value over S and S-E apex it probably caused by thicker crustal body with low density material.

5.2.4. Regional Gravity Anomaly Map

The regional anomaly (fig.5.6) separated from the residual anomaly map using second order polynomial fitting, it has contours interval of 5 mGal .It varies -90 to -210 mGal

The regional anomaly is dominated by SSE-NNE trend contour that has the highest value of the map .while the minimum anomalies observed at the upper corner of NW direction of the regional anomaly map and the intermediate gravity observed over SW-NW. Generally, the anomaly increment shows over NW-SE trend.

CHAPTER – SIX

6. GRAVITY MODELLING AND INTERPRETATION

6.1. Euler Deconvolution.

Euler deconvolution assists the interpreter by indicating portions of the data of interest, which can then be modeled in detail. No particular geological model is assumed; a range of elementary magnetic distributions such as point poles and dipoles are used as the source of the anomalies. The input is a magnetic, gravity, or analytical signal profile, and the output is a plot of the location of the different types of sources present.

Sources are characterized by their structural indices, which correspond to the rate of decay of the field strength with distance from the source. Some examples are given below;

Structural Index	Source Type
1.0	thin prism
2.0	line of dipoles
3.0	point dipole

Euler deconvolution can be applied in a wider variety of geologic situations than conventional model-dependant techniques. It has been applied to the residual data for selected profiles. For the extended Euler method, the first step involves solution of the one or more of the equation:

$$X_o \frac{\partial g}{\partial x} + Y_o \frac{\partial g}{\partial y} + \alpha = X \frac{\partial g}{\partial x} + Y \frac{\partial g}{\partial y} + ng$$

The left hand sides contain the unknowns i.e. source location (X_o, Y_o) and constant α. The right hand sides contain the known observation location (X, Y) where as n is the structural index and g is the field. **Fig.6.3**and **6.4** Show the outcome of the Euler method taken from the residual map of order 2 along the profiles.

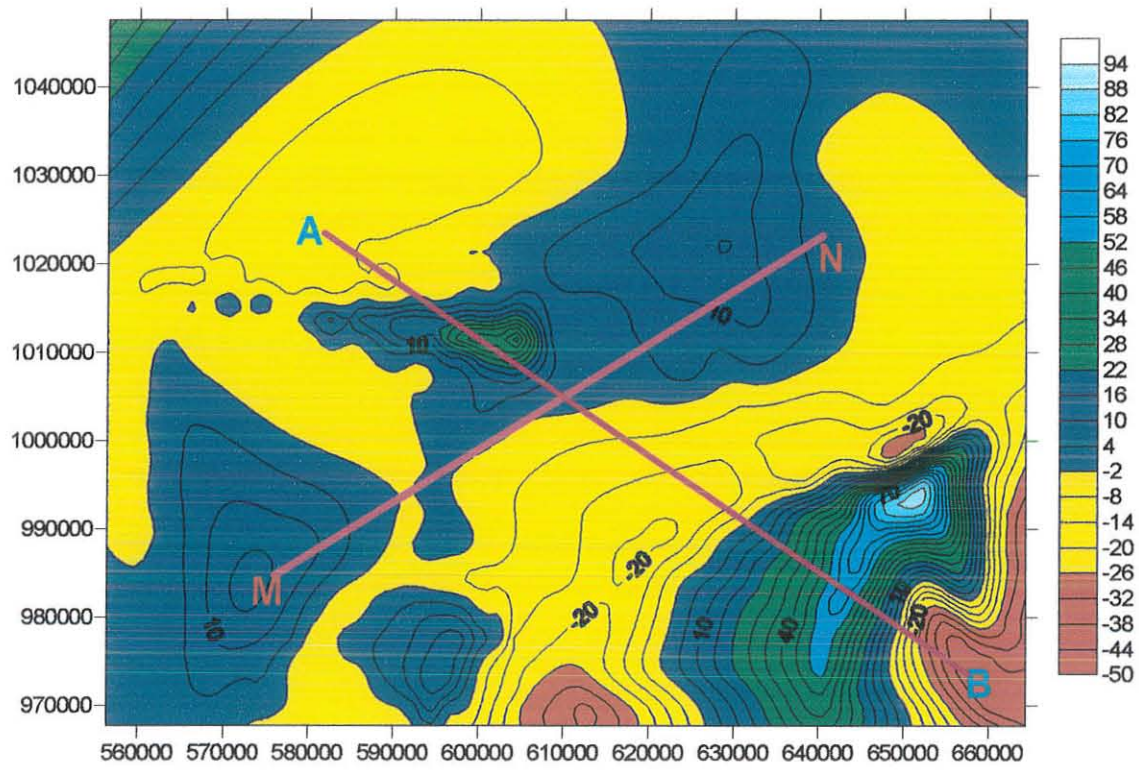

Figure 6.1. Profiles location on residual Bouguer anomaly of order 2

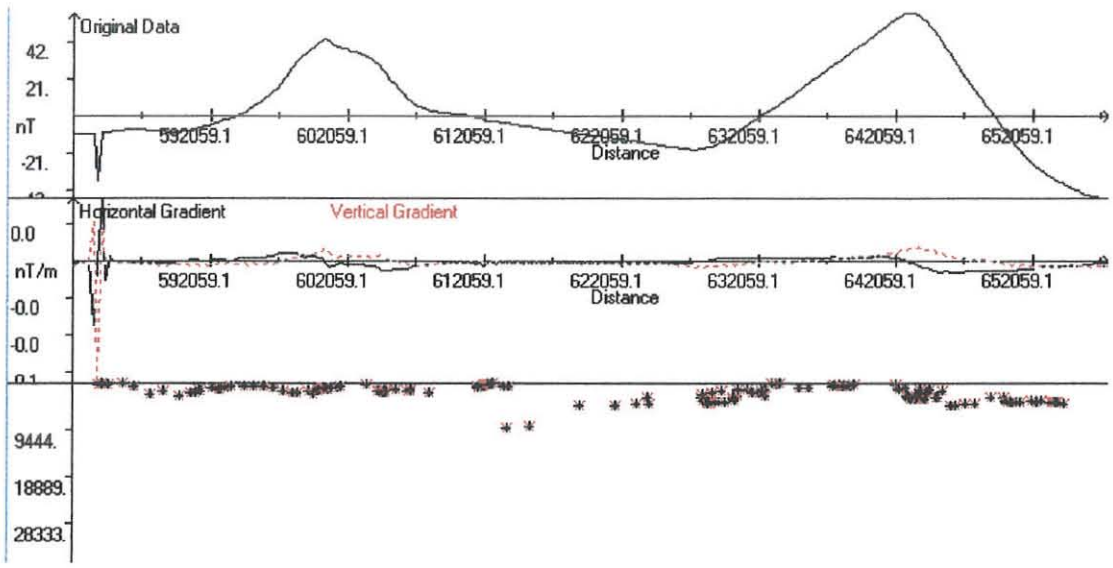

Figure 6.2. Euler deconvolution along profile AB.

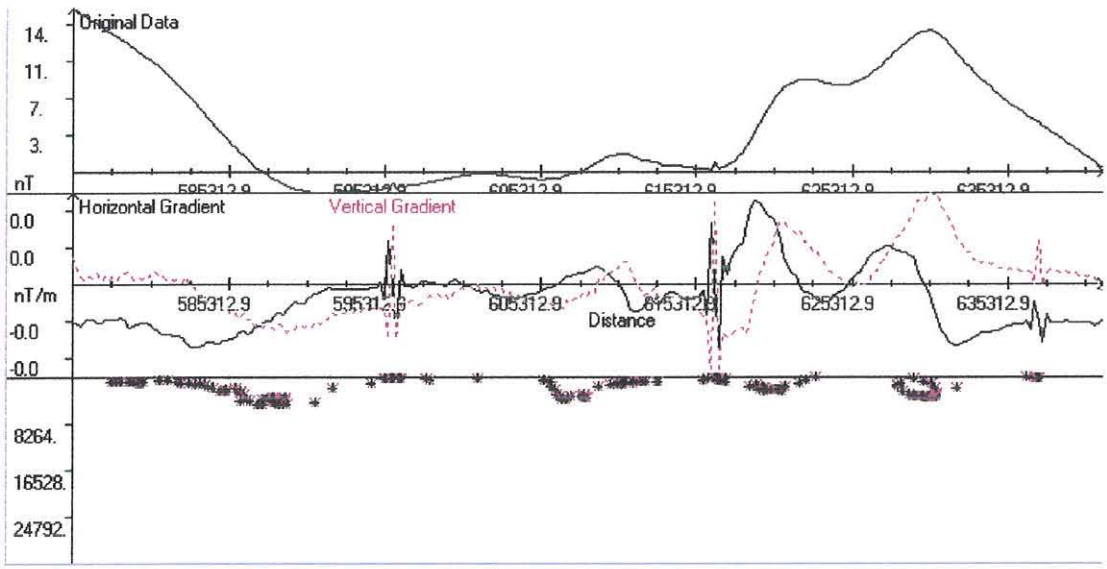

Figure 6. 2. Euler deconvolution along profile NM

6.2 MODELLING

There are two type of modeling. They are:-

1. Direct methods or **forward modeling** it is characterized by setting up a model, calculating the gravity anomaly and comparing it with the observed data and finally adjusting, the model until the data are fit well. The initial model may be attached through parametric measurements or geological.

2. Indirect methods or **inverse modeling** this involves the data to draw conclusions about the causative body for instance, the maximum depth to the top and the excess mass. Some parameters may be calculated, but the over all inverse problem (i.e. calculating the body from the anomaly) is inherently non unique

6.3. Initial Model

This initial model is obtained from previous study in title called '*crustal Velocity Structure across the Main Ethiopian Rift Results from Two-dimensional Wide-angle Seismic Modelling.*" (Geophys.J. Int.(2005)) and from Euler desconsolation along the selected profiles.

No	Rock type	Velocity(Km/s)	Density (Kg/m^3)	Thickness(m)
1	Volcanic sediment layer	4.1	2350-2560	3000-5000
2	Upper crust	6.1-6.45	2600-2700	7000-11000
3	Lower crust	6.6-7.2	2800-2980	15000-22000
4	Upper mantel	7.4-7.8	3100-3200	22000-29000

Table6.1 Initial model.

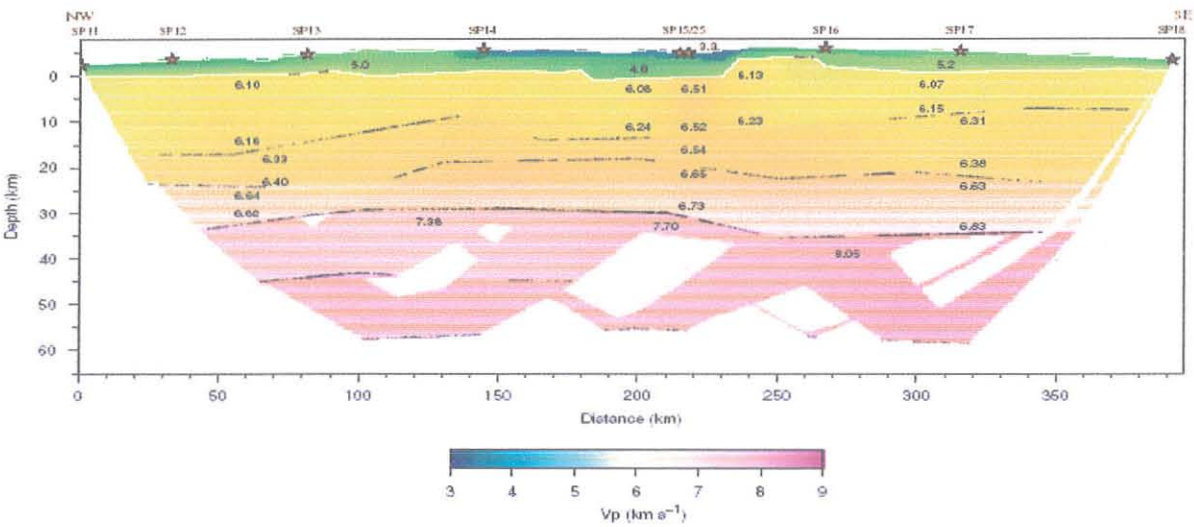

Figure .6.4. Two dimensional *P*-wave velocity model across the Ethiopian Rift (G.D Mackenzie, H.Thybo and P.K.H. Maguire, 2005). Black dots indicate wide-angle reflection points on seismic first-order discontinuities.
(Note that depth scale is relative to MSL.). And this model's profile was taken in the same orientation as profile AB (Fig.6.1).

6.4. 2.5 D forward modeling

In order to interprets the study quantitatively of the anomalous body using forward modeling for polygonal-shaped and 2.5-D bodies processed by a software called Grav2Dc (Cooper ,2003) depends on the Talwani algorithm (Talwani et al.1959) along the selected profiles.

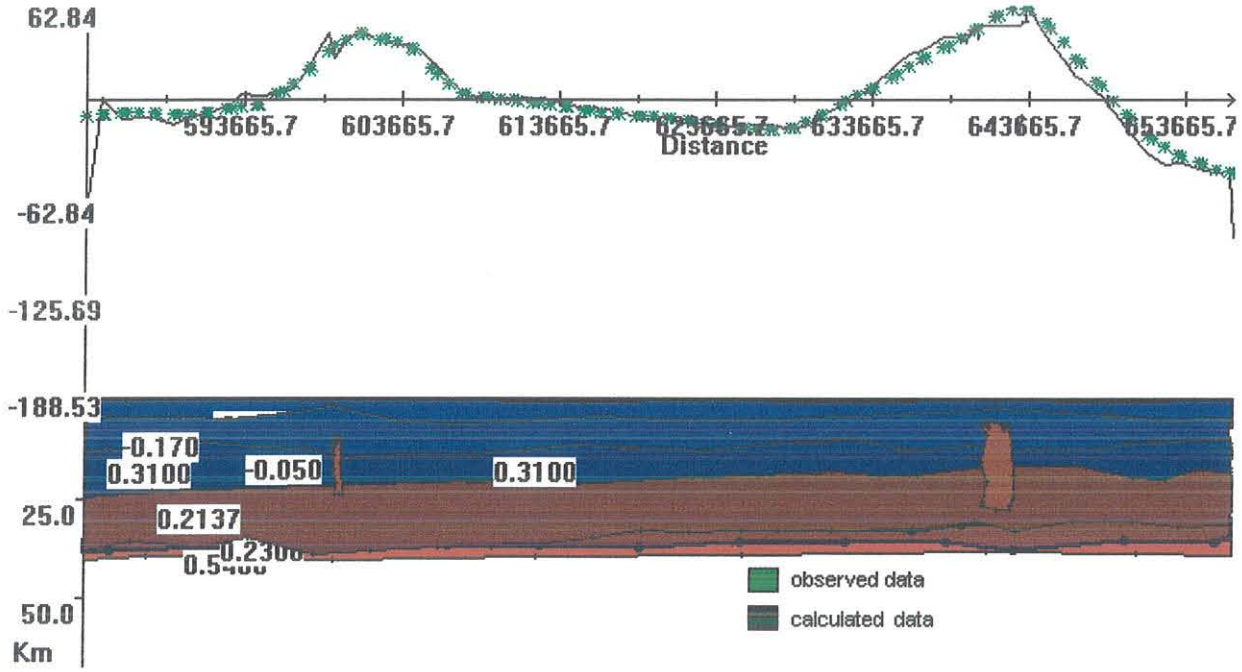

Figure 6.5. Model along profile AB

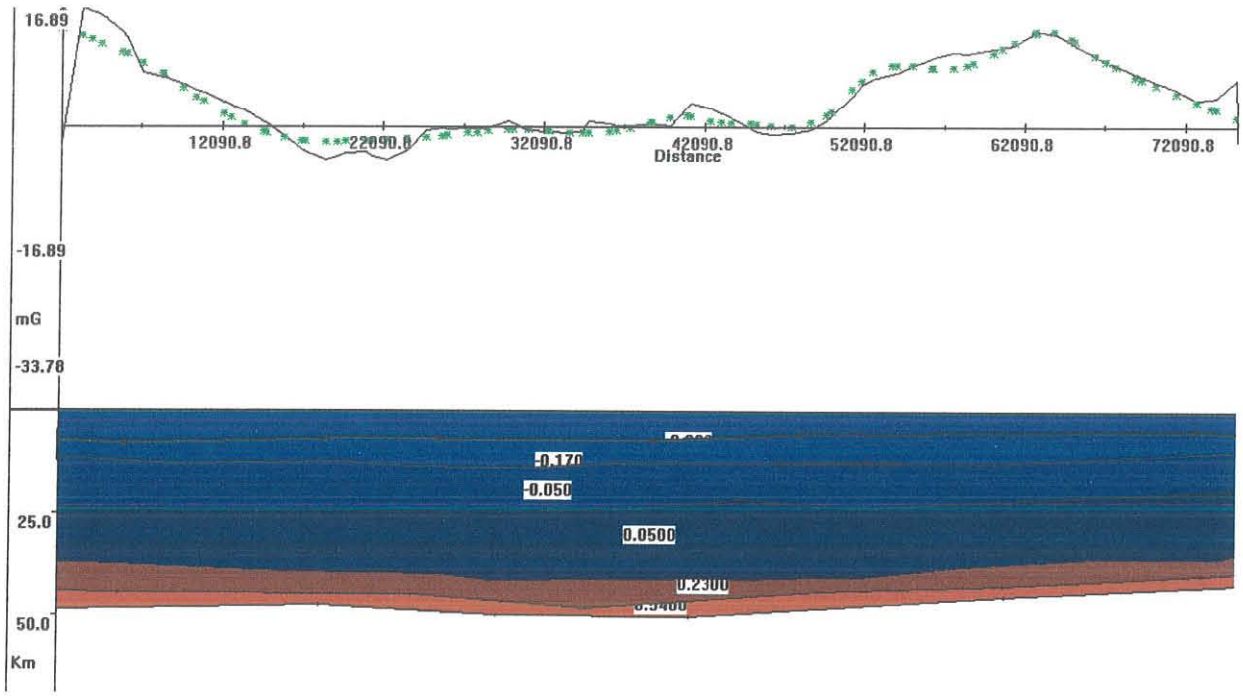

Figure 6.6. Model along profile MN

6.5. INTERPRETATION OF THE MODELES

6.5.1. Model along profile AB

This profile taken over the residual anomaly along which the higher positives anomaly effects are observed. The model which was made from this profile (AB) has different layers with different density contrast and depth.

The model under this profile has six layers and two anomalous bodies with high density contrast. The layer which is found over the surface has – 0.321 density contrast. Beneath this layer the model indicates layer which has a relatively higher density contrast from layer above it and its density contrast is –0.17 with depth at 2.66km. where as the other one which was modeled at a depth 7.69km with density contrast –0.05 value and 0.217 value density contrast with depth 11.54km was detected as a modeled layer of four and 0.23 density contrast layer hosted to layer above it at a depth of 34.802 km and its thickness varies over the profile. The layer which was modeled to be the lower one supposed to possess 0.54 density contrast at a depth of 39.173km.

The layers with –0.17 and –0.1 Density contrast have a contribution for the formation of the upper crust with relative depth of 7.7km deep. While the other two layers with appositive density contrast at 28.4km depth assumed to be lower crust. The two anomalous bodies with density contrast 0.31 values located at a depth of 11.98 and 13.905km respectively. These two bodies where probably assumed to be mafic intrusions.

Therefore, from this model one can observe the crustal thins to 34.8 km along the profile AB taken.

6.5.2. MODEL ALONG PROFILE MN

This profile (MN) which was taken over the residual anomaly map tri to show the most possible subsurface structure of the region

Here also the model shows six layers with different density contrast and different depth location over the profile taken. A very low density martial observed over the surface with density contrast –0.32, where as the second and third layer has –0.17 and –0.05 density contrast 4.44 and 9.17km at this given depths located respectively.

The layers up to 9.17km depth have a contribution for the upper crust structure and the relative higher denser materials are associated with layers those have 0.05 and 0.23 densities contrast accordingly with 16.57 and 36.6km depth location. And these two layers are supposed to form the lower crust of the region where the study conducted. The upper mantle of the model taken from this profile has the highest density contrast of 0.54 at 41.46km depth. This layer supposed to have a magmatic material associated with it. Then, from this model the crustal thickness is around 36.6km. Over the upper mantle.

CHAPTER-SEVEN

7. CONCLUSIONS AND RECOMMENDATIONS

7.1. CONCLUSIONS:-

After processing and interpretations of the measured data over the study area. Through qualitatively from different anomaly map and quantitatively using 2.5D forward modeling this was taken from the favorite profiles over the trend of the residual gravity map. Then, it will be concluding that from this study as:-

- The Residual anomaly map shows the highest positive gravity values and a condensed gradient observed. This trend is located at the lower corner of S-E part of the map and it may be caused by a plug type of structure or mafic intrusion.

- The higher gravity value is observed over N-E trend and its lower gravity value clearly observed over N-E apex part of the residual anomaly map.

- Depending on the models the crustal thickness is around 36.6km over the profile MN and 34.8km along the profile AB.

7.2. RECOMMENDATION

Based on the study that. I suggest that due to the ambiguity problems inherent in gravity method other geophysical methods such as seismic refraction should be done to justify the results.

References

Barberi, F., Varet, J.(1977) Volcanism of Afar: small-scale plate tectonics implication. Geological Society of America Bulletin 88:1251–1266.

Barberi, F., Bonati, E., Marinelli, G., Varet, J.(1974) Transverse tectonic during the split of continent: Data from the Afar rift. Tectonophysics 23:17–19.

Berhe, S.M., Desta, B., Nicoletti, M., Teferra, M.(1987) Geology, geochronology and geodynamic implications of Cenozoic magmatic province in W and SE Ethiopia. Journal of the Geological Society of London 144: 213–226.

Beyene and Abdelsalam (2005) Tectonics of the Afar Depression: A review and synthesis. Journal of African Earth Sciences 41: 41–59.

Fuchs, K., Altherr, R., Mueller, B., Prodehl, C. (Eds.)Structure and Dynamic Processes in the Lithosphere of the Afro-Arabian Rift System. Tectonophysics 278: 47–62

Cordell, L.(1979) Gravimetric expression of graben faulting in Santa Fe Country and the Espanola Basin, New Mexico: New Mexico. Geol. Sot. Guidebook, 30theField Conf., pp. 59-64.

Collet, B., Taud, H., Parrot, J.F., Bonavia, F., Chorowicz, J.(2000) A new kinematic approachfor the Danakil Block using a digital elevation model representation. Tectonophysics 316: 343–357.

Cooper, G.R.J.(2003a). Grav2dc, V.2.10 for Microsoft windows. School of Geosciences University of the Witwatersr and, Johannesburg, South Africa [Online].www.cooperg@geosciences.witz.ac.za

Courtillot, V.(1982) Propagating rifts and continental breakup. Tectonphysics 1: 239–250.

Courtillot, V., Achache, J., Landre, F., Bonhommet, N., Montigny, R., Feraud, G.(1984)Episodic spreading and rift propagation; new paleomagnetic and geochronologic data from the Afar nascent passive margin. Journal of Geophysical Research 89: 3315–3333.

Courtillot, V., Armijo, R., Tapponnier, P.(1987) Kinematics of the Sinai triple junction and a two phase model of Arabia–Africa rifting continental extensional tectonics. Geological Society Special Publications 28:559–573.

CNR-CNRS-Afar team. (1973) Geology of northern Afar (Ethiopia). Revue de Geographie Pysique et de Geologie Dynamique 2: 343–390.

Geographie Pysique et de Geologie Dynamique 2: 343–390.

DOBRIN, M.B., AND SAVIT, C.H.(1988) Introduction to Geophysical Prospecting. McGraw– Hill Inc. Singapore p. 630.

Ebinger, C.J., Casey, M.(2001) Continental breakup in magmatic provinces: an Ethiopian example. Geology 29: 527–530.

Ebinger, C.J., Sleep, N.H.(1998) Cenozoic magmatism throughout East Africa resulting from impact of a single plume. Nature 395: 788–791.

Ebinger, C.J., Yemane, T., WoldeGabriel, G., Aronson, J.L., Walter, R.C.(1993) Late eocene- recent volcanism and faulting in the southern Main Ethiopian Rift. Journal of the Geological Society of London 150: 99–108.

Ghebreab, W., Carter, A., Hurford, A.J., Talbot, C.J.(2002) Constraints for timing of extensional tectonics in the western margin of the Red Sea in Eritrea. Earth and Planetary Science Letters 200: 107–119.

Hofmann, C., Courtillot, V., Feraud, G., Rouchett, P., Yirgu, G., Ketefo, E., Pik, R.(1997) Timing of the Ethiopian flood basalt. Tectonophysics 141: 199-214.

Kazmin, V.G., Byakov, A.F.(2000) Magmatism and crustal accretion in continental rifts. Journal of African Earth Sciences 30: 555–568.

Makris, J., Ginzberg, A.(1987): The Afar depression: transition between continental rifting and sea-floor spreading. Tectonophysics 141: 199–214.

McKenzie, D.P., Davis, D., Molnar, P.(1970) Plate tectonics of the Red Sea and East Africa. Nature 226: 243–248.

Mickus .Ka,*, Ketsela Tadesse b, G.R. Keller b, Befekadu Oluma c (2007)Gravity analysis of the main Ethiopian rift. Journal of African Earth Sciences 48: 59–69

Mickus, K. L., and Peeples, W. J.(1992) Inversion of gravity and magnetic data for the lower surface of a 2.5 dimensional sedimentary basin: Geophysical Prospecting, 40, pp.171- 194.

Mohr, P.A.(1975) Structural setting and evolution of Afar. In: Pilger, A., Rosler, A. (Eds.), Afar Depression of Ethiopia, Proceedings of an International Symposium on the Afar Region and Rift Related Problems, Bad Bergzabren, Germany, 1974, vol.1. E. Schweizerbart_scheVerlagsbuchhandlung, Stuttgart, Germany, pp. 27–37.

Montenat, C., Ott d_Estevou, P., Purser, B.H. (1998) The Suez Rift and the north-western RedSea Neogene sedimentation and tectonic evolution. In: Purser, B.H.

(Ed.), Dynamics and Methods of Study of Sedimentary. Oxford and IBH Publishing Company, New Delhi, India, pp. 173–199.

Pallister, J.S.(1987) Magmatic history of Red Sea rifting; perspective from the central Saudi- Arabian coastal plain. Geological Society of America Bulletin 98: 400–417.

Sultan, M., Becker, R., Arvidson, R.E., Shore, P., Stern, R.J., El Alfy, Z., Guinness, E.A.(1992) Nature of the Red Sea crust: a controversy revisited. Geology 20:593–596.

Talwani, M, Worzel, JL, and Landisman, M.(1959) Rapid Gravity Computations for Two- Dimensional Bodies with Application to the Mendocino Submarine Fracture Zone, Journal of Geophysical Research, 64: 49-61.

Tefera, M., Chernet, T., Haro, W.(1996) Explanation of the Geological Map of Ethiopia. Ethiopian Institute of Geological Surveys, Addis Ababa, vol. 3, p. 79. Vail, J.R., 1985. Pan- African (late Precambrian) tectonic terrains and reconstruction of the Arabian–Nubian Shield. Geology 13: 839-842.

Telford, W.M., Geldart, L.P., and Sheriff, R.E.(1990) Applied Geophysics, Cambridge Univ.Press p.860.

Tessema.A*,L.A.G. Antoine (2004) Processing and interpretation of the gravity field of the East African Rift: implication for crustal extension. Tectonophysics 394: 87-110

Varet, J.(1978) Geology of Central and Southern Afar (Ethiopia and Djibouti Republic) F. Gasse .Eds. CNRS, France, Paris, p. 118.

White, R., McKenzie, D.(1989) Magmatism at rift zones; the generation of volcanic continental margins and flood basalts. Journal of Geophysical Research 94: 7685–7729

DECLARATION AND COPYRIGHT

I declare that this thesis is my original work and has not been prepared for any degree in any University, and that all the sources of materials used for the thesis have been duty acknowledged

Name: Addisu Guta.

Signature: _____

Place of submission: _____

Date: _____